

Functional Morphology and Virtual Models: Physical Constraints on the Design of Oscillating Wings, Fins, Legs, and Feet at Intermediate Reynolds Numbers¹

JEFFREY A. WALKER²

Department of Biological Sciences, University of Southern Maine, 96 Falmouth St., Portland, Maine 04103

SYNOPSIS. Why do some animals swim by rowing appendages back and forth while others fly by flapping them up and down? One hypothesis suggests the answer lies in the sharply divergent physical environments encountered by small, slow animals, and large, fast animals. Flapping appendages allow large animals to move through a fluid environment quickly and efficiently. As size and speed decrease, however, viscous drag increasingly dominates the force balance, with negative consequences for both rowing and flapping appendages. Nevertheless, comparative data suggest that flapping does not occur in animals at Reynolds numbers (Re) less than about 15. I used a computer simulation experiment to address the question, “Below what Re is rowing more effective than flapping?” The simulation, which employed a simple quasi-steady, blade-element model of virtual oscillating appendages, has several important results. First, the mechanical efficiency of both rowing and flapping decrease dramatically with scale. Second, the performance of rowing can increase substantially by taking advantage of several dynamic shape modifications, including area and span reduction during the recovery stroke. Finally, the relative performance of rowing and flapping is dependent on the advance ratio, which is a function of the travel speed relative to the oscillation frequency. The model predicts that rowing is more efficient than flapping at $Re < 20$ for animals moving throughout the range of typically observed advance ratios.

INTRODUCTION

The dynamic shape of propulsive appendages in animals that swim or fly varies from a rowing (or paddling) motion that is largely parallel to the direction of travel to a flapping motion that is largely normal to the direction of travel. Rowing and flapping occur in diverse taxonomic groups, including at least three different phyla, and have independently evolved numerous times. Why do some animals row while others flap? Several explanations have been proposed (Fish, 1993, 1996; Vogel, 1994; Walker and Westneat, 2000) but this paper focuses on one, the scaling hypothesis, which suggests that because of the increasing dominance of viscous forces relative to inertial forces at small scales, small, slow animals should row their appendages because rowing appendages can exploit viscous forces to generate thrust while flapping appendages cannot (Horridge, 1956; Bennett, 1972; Daniel and Webb, 1987).

The consequences of the physical properties of fluids on locomotor performance are highly scale dependent. For the purpose of biological fluid dynamics, scale is represented by the dimensionless Reynolds number (Re), a ratio that reflects the influence of inertial relative to viscous forces. Biologically inspired discussions of Re are found in Denny (1988) and Vogel (1994). Re is computed by $Re = LU/v$, where L is some relevant length, U is the velocity of the fluid relative to the object, and v is the kinematic viscosity of the fluid. The Re that I will discuss are in the range 1 to 100, which is biologically intermediate but will

be referred to as low, since they are at the low end of the intermediate range (Daniel and Webb, 1987; Daniel *et al.*, 1992). Re above 100 will be referred to as high, simply for convenience. For comparison, the Re of the hand of an Olympic athlete swimming the breaststroke at 1.67 m/sec is 1.4×10^5 in fresh water but only 5 in corn syrup.

To understand the problem of generating thrust from an oscillating appendage at low Re , it is useful to review the function of airfoils at high Re . At high Re , an airfoil that is tilted, or pitched, relative to the oncoming fluid (air or water) experiences a resultant force that is largely normal to its surface (Fig. 1). Lift is the component of the resultant force that is normal to the flow while drag is the component parallel to the flow. The angle of the airfoil relative to the flow is the angle of attack. At small attack angles, the fluid smoothly flows over the leading edge of the airfoil but separates from the surface near the trailing edge. The separation creates a small region of low pressure that sucks in passing fluid creating an unstable vortex that eventually sheds into the wake. Above a threshold attack angle (12° – 18°), the fluid separates from the surface of the airfoil as it passes the leading edge creating a large leading edge vortex (Freymuth, 1988; Dickinson and Götz, 1993; Dickinson, 1996). The leading edge vortex is not simply a phenomenon of human engineered airfoils but, in fact, has been verified on the flapping wings of the hawkmoth *Manduca sexta* (Ellington *et al.*, 1996). After a short time, the leading edge vortex grows to an unstable size and sheds into the wake. The resultant force includes a component due to the bound circulation and a component due to the presence of the vortex itself; consequently, the resultant force is larger than that expected given the bound circulation alone (Dickinson and Götz, 1993).

¹ From the Symposium *Molecules, Muscles, and Macroevolution: Integrative Functional Morphology* presented at the Annual Meeting of the Society for Integrative and Comparative Biology, 3–7 January 2001, at Chicago, Illinois.

² E-mail: walker@usm.maine.edu

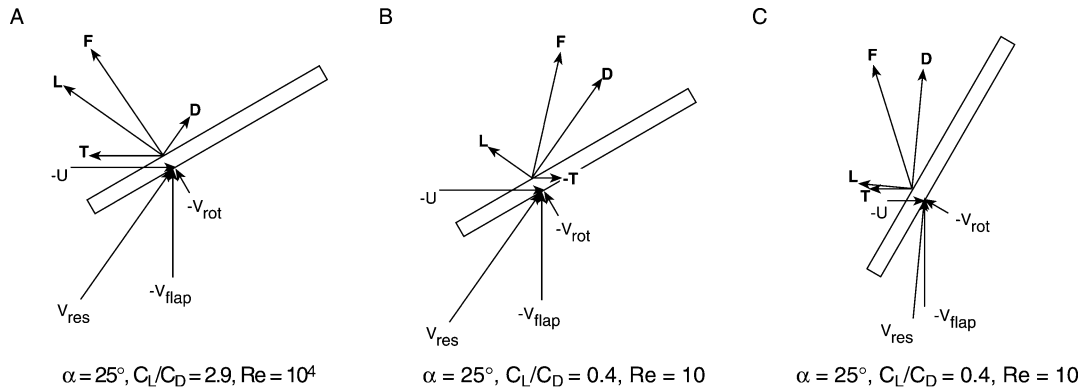


FIG. 1. Aerodynamic forces on flapping plate at different scales. The plate is translating to the left with speed, U , flapping down with speed V_{flap} , and rotating clockwise about a point near its leading edge, resulting in the tangential velocity at the center of pressure, V_{rot} . In (A) the plate is pitched 30° and the scale is high Re . Thrust, T , has a small angle to lift, L , hence the thrust is “lift-based.” (B) has the same kinematics as (A), only the scale is at low Re . Because of the low C_L/C_D , the resultant force, F , is tilted back to the trailing edge, resulting in negative thrust. In (C), the flapping and rotational speeds are the same as in (A) but the plate is pitched 60° and the translational speed is 30% of that in (A). Despite the low Re , the plate generates positive thrust. Note that the upward force, which is important for flying or negatively buoyant animals, is due largely to drag, D .

At high attack angles, large vortices separate over both edges, resulting in a very characteristic signature of pressure drag, the von Kármán vortex street (Frey-muth, 1988; Dickinson, 1996). While a stationary airfoil cannot generate thrust, an oscillating airfoil can if heaving (the translational movement) and pitching (the rotational movement) have the correct phase relationship. A heaving and pitching airfoil that generates thrust creates a signature wake called a reverse von Kármán vortex street (Frey-muth, 1988; Dickinson, 1996; Anderson *et al.*, 1998).

At small angles, when no leading edge vortex is present, the force due to the bound circulation is the bound circulatory force. At very high angles of attack, the presence of the attached vortex is called pressure drag, since it is largely parallel to the flow. The combined force due to bound circulation and presence of an attached vortex has no name, although Kuethe (Kuethe and Chow, 1986) calls the lift component of this combined force “vortex lift.”

Flapping works by generating forces that are largely normal to the flows over the appendage, hence flapping is often thought of as “lift-based” (Fig. 1). By pitching the appendage leading edge down on the down stroke (negative pitch) and leading edge up on the up stroke (positive pitch), a flapping appendage can generate thrust throughout the stroke cycle. All flying animals, regardless of phylum (Arthropoda, Mollusca, or Chordata) or fluid medium (air or water), flap with this geometry (although animals flying in air may reduce upstroke loading, and its drag or negative lift component, by feathering their wings (Tobalske, 2000)). Flapping works at high Re because, at this scale, the bound circulatory and vortex forces are large (Dickinson, 1996).

In rowing, forces are largely parallel to the resultant flow vector, which is why rowing is often referred to as “drag-based,” although the acceleration reaction is also an important component of the thrust balance

(Daniel, 1984). Rowing works by creating an asymmetry in the stroke geometry. Oscillating the appendage about a spanwise axis that is directed posterolaterally creates an asymmetry that allows the acceleration reaction to generate net thrust (Daniel, 1984). Feathering the appendage during the recovery stroke creates an asymmetry that allows larger drag on the power stroke (felt as thrust at the center of mass) than recovery stroke. Rowing with a feathered recovery stroke works at high Re because at this scale the drag on an appendage that is oriented with its surface normal to its motion is much higher than the drag on an appendage that is oriented with its surface parallel to its motion.

As animals get smaller and move more slowly (that is, as scale, or Re , decreases), the importance of inertial forces relative to viscous forces on propulsive appendages decreases, which has three consequences. First, the bound circulation decreases. Second, viscous (skin-friction) drag sharply increases. Third, at small enough scales, fluid passing over an appendage will fail to separate. The failure to separate not only effects pressure drag but also circulatory lift because the augmented vortex lift mechanism outlined above is dependent on this separation. As scale decreases, viscous forces inhibit separation with the consequence that the additional lift must diminish and, at some unknown Re , disappear.

At high Re , lift is much higher than viscous drag, and the resultant force on a flapping appendage will largely be normal to its surface. As Re falls, lift decreases, viscous drag increases and the resultant force tilts more toward the trailing edge (Fig. 1). The ability of a flapping appendage to generate thrust from lift, then, depends on the ratio of lift to drag, which decreases dramatically as Re decreases (Fig. 2).

A rowing appendage can potentially exploit the large viscous forces occurring at low Re (by generating large skin friction drag on the power but not recovery

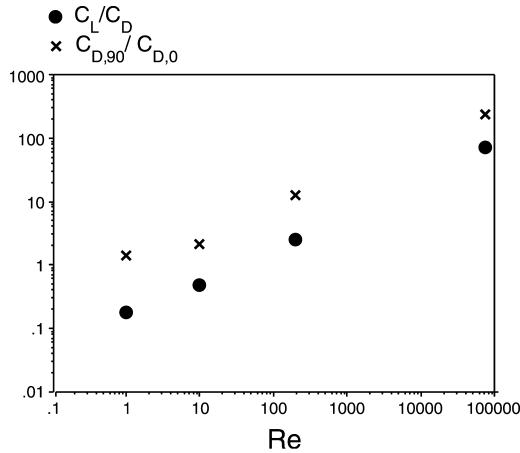


FIG. 2. The change in (A) maximum C_L/C_D and (B) $C_{D,90}/C_{D,0}$ with scale (Re). Data from Thom and Swart (1940), Dickinson and Götz (1993) and Shyy *et al.* (1999).

stroke), so we might think that, *a priori*, rowing is more effective than flapping at low Re . The problem with rowing at low Re is the failure of fluid to separate from the appendage’s surface, with the consequence that the drag on an appendage oriented at 90° to the flow is not much more than the drag with the appendage oriented 0° to the flow (Fig. 2) (Vogel, 1994). Consequently, feathering will not be able to produce the asymmetry necessary for the rowing appendage to generate net thrust (Norberg, 1972).

COMPARISON OF ANIMALS THAT ROW AND FLAP AT INTERMEDIATE Re

While several authors have argued that lift-based flapping should be ineffective at Re less than 100 (Horridge, 1956; Bennett, 1972; Webb and Weihs, 1986; Daniel and Webb, 1987) the qualitative analysis above suggests that rowing may not be any better. A comparison of animals that row or flap can suggest which dynamic shape, rowing or flapping, is more ef-

fective at low Re (Table 1). The Re values in Table 1 were computed using the mean flapping velocity at the appendage tip and the mean or maximum chord. The available data show that rowing occurs throughout the range of biologically intermediate Re while flapping is restricted to $Re > 10$. For neutrally buoyant animals, the table suggests that flapping is restricted to $Re > 100$.

The minimum Re for flapping appendages should be accepted cautiously because there are few data on the most relevant animals, including fishes, pteropods and small insects. Large pteropods, including *Clione limacina* and *Cymbulia peroni*, employ the stereotypical flapping motion to hover and swim across a range of speeds at $Re > 100$ (Satterlie *et al.*, 1985, 1997; Davenport and Bebbington, 1990; Harbison, 1992). While the best quantitative data are on larger individuals, Morton (1958) illustrated the flapping stroke of a small *C. limacina* (wing length less than 1 mm). No frequency was reported; with a frequency of 5 Hz, the wings of this small individual would be operating at a Re of about 15. The wings of the small thecostomatous pteropod, *Limacina retroversus*, operate at even smaller Re , between about 1 and 10 (Walker, unpublished data). The dynamic shape of the wings of *L. retroversus* has been qualitatively described as having a vertically oriented rowing motion, with a downward power stroke and upward recovery stroke, that generates net upward forces (Morton, 1954).

Because of the small C_L/C_D at low Re , it has been suggested that the wings of the smallest flying insects, including members of the Mymaridae (Hymenoptera), Trichogrammatidae (Hymenoptera) and Ptiliidae (Coleoptera), operate at $Re < 10$ and move with a modified “rowing” geometry, perhaps not unlike that of *L. retroversus* (Thompson, 1917; Horridge, 1956; Bennett, 1972). While there is no experimental work on the smallest insects to verify this hypothesis, Weis-Fogh, (1973) has shown that the tiny wasp *Encarsia formosa* (wing length approximately 0.6–0.7 mm),

TABLE 1. Reynolds numbers (Re) for a representative group of animals that row or flap at biologically intermediate Re .*

Name	Common name	Dynamic shape	Re	Source
<i>Bosmina longirostris</i>	water flea	row	0.2–3.6	(Zaret and Kerfoot, 1980)
<i>Speleonectes lucayensis</i>	remipede crustacean	row	2	(Kohlhage and Yager, 1994)
<i>Artemia</i> sp.	brine shrimp	row	2.0–20	(Williams, 1994)
<i>Gnathopausia ingens</i>	mysid shrimp	row	64–125	(Hessler, 1985)
<i>Daphnia magna</i>	water flea	row	63	(Kohlhage, 1994)
<i>Acanthocyclops robustus</i>	copepod	row	70	(Morris <i>et al.</i> , 1990)
<i>Pleuromamma xiphia</i>	copepod	row	350	(Morris <i>et al.</i> , 1985)
<i>Cenocorixa bifida</i>	backswimmer	row	484	(Blake, 1986)
<i>Encarsia formosa</i>	wasp	flap	17	(Weis-Fogh, 1973)
<i>Clione limacina</i>	sea butterfly	flap	81–434	(Satterlie <i>et al.</i> , 1985; Satterlie <i>et al.</i> , 1997)
<i>Drosophila melanogaster</i>	fruit fly	flap	160–220	(Ennos, 1989)
<i>Simulium</i> sp.	black fly	flap	450	(Ennos, 1989)
<i>Ceriatrion melanurum</i>	damsel fly	flap	500	(Sato and Azuma, 1997)
<i>Vampireuthis infernalis</i>	vampire “squid”	flap	160–14,000	(Seibel <i>et al.</i> , 1998)
<i>Cymbulia peroni</i>	sea butterfly	flap	1,800–20,000	(Harbison, 1992)
<i>Callinectes sipididus</i>	blue crab	flap	13,000	(Plotnick, 1985)

* The Re were computed using the mean or maximum chord and the flapping velocity at the distal tip of the oscillating appendage.

which is about 3 to 4 times larger than the smallest flying insects, flies with a largely dorsoventrally oriented, flapping stroke during both fast forward flight and hovering. During hovering the Re is about 17 (Weis-Fogh, 1973).

Inferring the relative effectiveness of rowing and flapping using the comparative data is confounded by differences in the direction of optimal force production. That is, neutrally buoyant animals need only generate thrust while negatively buoyant animals need to generate both thrust and upward forces. "Lift-based" flapping is a better geometry for generating the combination of thrust and upward forces, hence pteropods and tiny insects, both of which are negatively buoyant, may use a flapping mechanism even though it is more costly or less effective than a rowing mechanism for generating thrust at low Re . The data in Table 1 suggest that for nearly neutrally buoyant animals, rowing is the exclusive propulsive mechanism for oscillating appendage propulsion at $Re < 100$.

METHODS OF MORPHOLOGY-PERFORMANCE INFERENCE

The comparative method

How does one test for a causal relationship between morphology (in this case, the dynamic shape of an oscillating appendage) and performance (ability to swim at low Re)? The comparative method, the most common tool for inferring causal relationships between morphology and performance, exploits manipulations provided by nature. Unfortunately, nature neither controls confounding variation nor randomizes individuals among treatments. High correlations between morphology and performance may create the illusion that the focal morphology directly influences performance. Indeed, several experimental phenotypic manipulation studies have failed to support causal hypotheses of performance variation based on comparative data (Jayne and Bennett, 1989; Olsson *et al.*, 2000; Srygley and Kingsolver, 2000; Veasey *et al.*, 2000).

There are two potential problems with the comparative method for inferring causal relationships between morphology and performance. First, a morphology that is a factor may show no correlation because other characters mask its effect (analogous to Type II errors in statistics). Second, morphologies that have no effect on performance may be spuriously correlated with performance because of phenotypic correlation with the actual factors (analogous to Type I errors in statistics). The first type of error occurs when a trait performs multiple roles and optimizing the trait for one role decreases its performance for another. This is the classic source of phenotypic trade-offs. Compensation by other structures may maintain high performance, despite the locally "suboptimal" morphology (Sinervo *et al.*, 1991; Endler, 1995; Law and Blake, 1996).

The second type of error occurs because species differ in numerous traits; some of these affect the performance of interest but most do not. These errors are

most problematic in two species comparisons (Garland and Adolph, 1994) but even phylogenetically correct, multi-species comparisons (Garland and Adolph, 1994) do not escape the problem that mechanisms are inferred from statistical associations (Endler, 1986; Jayne and Bennett, 1989; Leroi *et al.*, 1994). Inferring causation from a correlation among many data points (either individuals within a population or species within a clade) assumes that phenotypic differences other than the ones relevant to the study are randomized among the cases and only variables that causally affect performance will have high correlations with performance. Both correlated stabilizing selection within populations and correlated directional selection among populations and species could produce spurious correlations.

Despite these cautions, comparative analyses of morphology and performance are valuable for two reasons. First, because variation among real organisms is what ultimately needs explaining, an exploratory comparative analysis should stimulate both modeling and phenotypic manipulation experiments. Second, confirmatory comparative analyses are necessary to test specific predictions generated by the results of a modeling or phenotypic manipulation experiment. For example, a comparison of the behavior of wrasses on the reef (Bellwood and Wainwright, 2001; Fulton *et al.*, 2001) and of laboratory measures of swimming performance among different species of wrasse (Walker and Westneat, 2002) supported the predictions generated by the simulation experiment of rowing and flapping fins at high Re (outlined below).

Phenotypic manipulation experiments

Phenotypic manipulation experiments (Sinervo and Basolo, 1996) allow a powerful means of inferring causation between morphology and performance but are uncommon in the performance literature relative to comparative analyses. While phenotypic manipulation should be implemented more frequently, two problems with phenotypic manipulation experiments that preclude their widespread use are treatments that are unethical and treatments that are impractical or impossible. For example, there are no phenotypic manipulation experiments directly addressing rowing versus flapping because it is difficult to force an animal to use one stroke or another. One possibility would be to measure performance of the same animal at different Re by manipulating the kinematic viscosity of the fluid (Fuiman and Batty, 1997; Johnson *et al.*, 1998).

Modeling experiments

Manipulation of modeled phenotypes or physical environments allow experiments that are unethical, impractical, or impossible on real animals. In a virtual, or software model, the geometry and kinematics of the morphological structure, as well as the physical environment relevant to the dynamics of the system, are modeled by mathematical functions. Treatments are experimentally manipulated by modifying these func-

tions. Simple virtual models can produce results very quickly, which allows an investigator to explore a large, densely sampled parameter space (combinations of treatments). Physical, or hardware, models are made from nuts and bolts, or anything else that can be purchased from a hardware store. A physical model operates in a real physical environment, so the environment is not necessarily modeled, although some environmental manipulations may be used to model the environment. Treatments are manipulated by modifying the shape of a structure, the software controlling the hardware's motion, and the physical environment (Archer *et al.*, 1979; Kingsolver and Koehl, 1985; Emerson and Koehl, 1990; McHenry *et al.*, 1995; Ahlborn *et al.*, 1997; Anderson *et al.*, 1998; Dickinson *et al.*, 1999; Kato, 1999). Sometimes only the physical environment is manipulated, and performance is measured on a real animal (Farley and McMahon, 1992; Fuiman and Batty, 1997; Johnson *et al.*, 1998; Chai *et al.*, 1999). In some cases, environmental manipulations are a proxy for phenotypic manipulations. For example, to make an animal that is moving in a fluid "smaller" or "larger," one can simply manipulate the kinematic viscosity of the surrounding fluid (Fuiman and Batty, 1997; Johnson *et al.*, 1998; Chai *et al.*, 1999).

VIRTUAL MODEL OF ROWING AND FLAPPING APPENDAGES

Summary of the model and the high Re experiment

A virtual model of oscillatory appendage propulsion was recently developed and used in a computer simulation experiment in order to compare rowing and flapping performance for appendages operating within a Re range between about 10^2 and 10^6 (Walker and Westneat, 2000). Two performance variables were estimated: the mean thrust over one half or one full stroke cycle and the mechanical efficiency of the full stroke cycle. Each appendage was modeled as a rectangular plate that articulated with the body at either 90° or 0° relative to the horizontal, depending if it was a rowing or flapping appendage, respectively. Appendages dynamically twisted down their span, which pitched the distal parts of the appendage relative to the base. The maximum pitch at any point along the span is the pitch amplitude and was modeled to vary linearly from base to tip. Two rowing kinematics were investigated. The untwisted rowing appendage rotated at its base causing the appendage to oscillate as a stiff plate. During the recovery stroke, the appendage pitched -90° , which rotated the appendage into a feathered orientation along its entire span. In the twisted rowing appendage, the base was not allowed to rotate and, consequently, the appendage twisted along its span during the recovery stroke. For both rowing models, the appendage rotated back to 0° pitch at the beginning of the power stroke. The orientation of the flapping appendage was fixed at its base but dynamically twisted throughout the stroke cycle. For both the

twisted rowing appendage and the flapping appendage, pitch amplitudes were optimized to find the peak mechanical efficiency (see below).

Forces on the virtual appendages were computed using a blade-element model. Blade-element models divide a propulsive structure into a series of blade elements, divide the stroke cycle into a series of discrete times, and compute a force balance on each element at each time. The total force on the appendage at a particular point in the stroke cycle is simply the sum of the elemental forces. In the computer simulation, the force on each blade element was modeled as the sum of a combined vortex-bound circulation-skin friction force and an inertial force, which included only an added mass, or acceleration reaction, component.

Two performance variables that are relevant to animal locomotion were computed: mechanical efficiency, η , and mean thrust, T_{avg} . An oscillating appendage accelerates fluid in many directions but only the backward component of the fluid acceleration is useful (resulting in thrust). Therefore, only a fraction of the energy transferred from the appendage to the fluid is useful; η , the ratio of useful work to total work, is a measure of this fraction. Animals that frequently engage in high endurance behaviors, such as continuous foraging at intermediate to high speeds, active defense of a territory, or migration, should use a stroke shape that maximizes η . Efficiency is probably most important for steady swimming. For maneuvering behaviors such as forward accelerations, braking, and turning, T_{avg} is more relevant because it is directly related to the force available for a maneuver.

The initial results of the model (Walker and Westneat, 2000) show that at $Re > 100$, flapping is more mechanically efficient than both twisted and untwisted rowing appendage regardless of swimming speed. In contrast, a rowing appendage generates more thrust than a flapping appendage at slow to intermediate speeds. Importantly, at low forward speeds, the η difference, or premium, between rowing and flapping is small but the T_{avg} premium is large. As speed increases, the η premium increases while the T_{avg} premium decreases and even reverses sign. The power required to balance body drag, or parasite power, increases with the cube of forward speed. This is important because the increased energy savings of flapping at low speeds may not offset the advantages of being able to generate large forces for maneuvering. As speed increases, however, the η premium becomes more important not only because the premium itself increases, but also because of the high parasite power. The model predicts that, in the absence of other constraints (such as the need for lift or terrestrial locomotion), slow, maneuvering animals should row and fast animals should flap.

Model predictions are informative only if the model assumptions and simplifications do not seriously bias the results. A comparison of the oscillating appendage model at high Re (>100) with relevant rowing and flapping physical models demonstrated that the virtual

model predicts the major features of oscillating appendage performance, including measures of mechanical efficiency, optimal twist amplitudes, optimal reduced frequencies and optimal Strouhal numbers (Walker and Westneat, 2000). The usefulness of any model lies in its ability to make predictions and explain variation. The results of the high Re experiment were consistent with observed patterns of rowing and flapping among many swimming animals (Walker and Westneat, 2000) and correctly predicted the relative swimming performance between closely related fishes from the family, Labridae (Walker and Westneat, 2002).

A model of low Re rowing and flapping

In order to explore the performance of rowing and flapping at low Re , we need a model of the change of lift and drag coefficients with Re . Data from Thom and Swart (Thom and Swart, 1940) were used to derive the equations

$$C_D = (1.86 + 13.75Re^{-1}) - 0.5 \cdot (1.74 + 3.86Re^{-1}) \\ \times \cos(2\alpha) - 0.3 \\ C_L = (1.14 + 1.62Re^{-1}) \cdot \sin(2\alpha)$$

for 2-D (infinitely long) flat plates at angle of attack α and $Re < 10$. At $Re = 200$, C_D and C_L were computed from a Fourier series fit to data representing the forces on a 2-D flat plate seven chord lengths after an impulsive start (Dickinson and Götz, 1993). For Re between 10 and 200, the coefficients were linearly interpolated between the two models (Thom and Swart, 1940; Dickinson and Götz, 1993). The 3-D coefficients used in the high Re model (Walker and Westneat, 2000) include the influence of induced drag. The induced velocity component was not included in this low Re model with the result that the 2-D C_L/C_D ratios are larger than their equivalent 3-D ratios at angles of attack less than 24° and smaller than the 3-D ratios at angles greater than 24° . For each element at each point in the stroke cycle, the input force coefficients were based on the instantaneous Re in addition to the angle of attack.

The low Re model was applied to rowing and flapping appendages with a rectangular planform, aspect ratio of 4, and constant forward speeds between 1 and 10 span lengths per second. For the rowing appendage, The stroke angle was held constant at 120° for the rowing appendage but optimized over the range 40° to 160° for the flapping appendage. The constant speed may be somewhat unrealistic at the lowest Re analyzed, especially for the rowing stroke, because travel speed can vary substantially between power and recovery strokes (Williams, 1994). A simple model with the swimming speed varying in phase with appendage angular velocity was explored but the results were not sufficiently different to warrant inclusion in this study.

Importantly, no constraints were applied to the optimization. For example, parasite drag from a virtual

body was not modeled, hence the results reflect the maximum performance of the appendages; to achieve this, an animal would have to have a body with a drag that balanced the mean thrust over the stroke cycle (In all cases, the thrust produced exceeded the theoretical drag that would occur on a spheroidal animal with length equal to limb span and breadth equal to length/4). Additionally, the optimization did not account for the muscle power available for oscillating the appendage at the optimal frequency and stroke angle.

Figure 3 shows the mechanical efficiency, η , as a function of Re and advance ratio, J , which is the forward speed standardized by flapping velocity (Ellington, 1984). For comparison, Ellington (1984) defined hovering in insects as $J < 0.1$. Typical J for forward swimming at $Re < 500$ ranges from 0.1 to 0.6. One exception is the remipede crustacean *Speleonectes lucayensis*, which rows with multiple pairs of legs, each at a Re of about 2 and a $J > 1$ (Kohlhage and Yager, 1994). Note that the Re for a stroke cycle was computed by averaging over all blade elements and time intervals. At low J , the averaged Re will be about half the mean-flapping-velocity Re (those in Table 1) while at high J , the averaged Re will approximate or even exceed the mean-flapping-velocity.

Rowing and flapping appendages are able to generate thrust, as indicated by the positive η , at all Re investigated. Re has a strong influence on η for both rowing and flapping appendages, although its effect diminishes with Re (the decreased slope cannot be fully appreciated on the logarithmic axis). J has a strong influence on mechanical efficiency with the consequence that the relative performance between rowing and flapping is strongly dependent on the combination of Re and J .

At the lowest Re , the root-rotating rowing appendage does not enjoy a substantially higher η than the twisted rowing appendage, a pattern predicted by the change in $C_{D,\alpha=90^\circ}/C_{D,\alpha=0}$ with decreasing Re (Fig. 2). Because the root-rotating rowing appendage is a better model than the spanwise twisting rowing appendage for animals swimming at low Re (with the possible exception of *Limacina retroversa*), all further manipulations of the rowing model used the root-rotating geometry (see below for a description of the manipulations).

The flapping appendage generated thrust with higher efficiency than the root-rotating appendage at all Re between 1 and 100 and J between 0.1 and 1 (Fig. 3). To generate positive thrust throughout the range of advance ratios found in animals moving at $Re < 100$ (that is, $J < 1$), the flapping appendage must operate above $Re 10$. Nevertheless, the quasi-steady flapping appendage is effective down to at least $Re 1$. How can the flapping appendage generate thrust at these low Re ? The answer is not surprising given the geometry of the flapping stroke allowed by the simulation (Fig. 1C). The simulation modeled the ideal case where the flapping appendages did not need to generate an upward force to balance the weight of the animal. Given

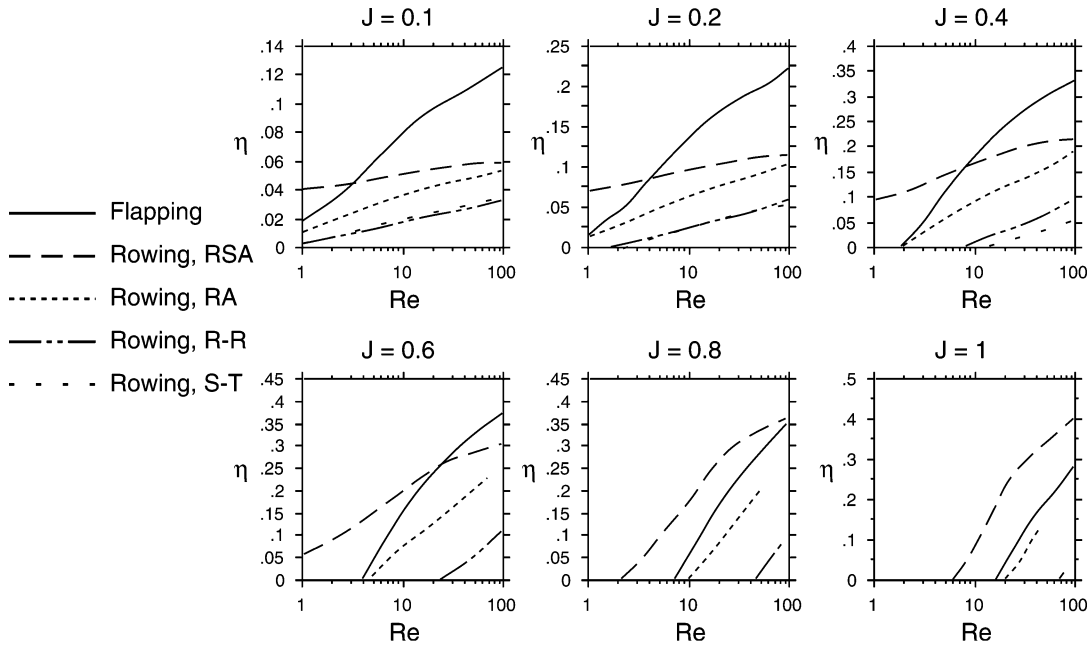


FIG. 3. The effect of Re and J on the performance, η (mechanical efficiency), of appendages that are flapping, rowing with reduced recovery stroke span and area (RSA), rowing with reduced recovery stroke area (RA), rowing with root-rotating geometry (R-R), and rowing with spanwise-twisting (S-T) geometry.

the vertical stroke plane, an optimal twist amplitude of approximately 83° per unit span, and a small advance ratio, most of the resultant flow at any point along the span is due to the flapping component, with the result that angles of attack are positive (nose up relative to velocity vector) on the downstroke and negative on the upstroke. Even with very small C_L/C_D , this geometry produces net positive thrust (as long as J is very low) (Fig. 1C). Importantly, however, the simulation sug-

gests an animal could not move very fast with a flapping stroke at Re near 1, unless it could oscillate its appendages rapidly, which should be limited by muscle power.

The superior performance of the flapping appendage is surprising and reflects two features of the model. First, the lack of constraints on the optimal flapping kinematics probably produced optimistic results for the flapping appendage. Details of the effects of stroke angle and pitch amplitude for the flapping stroke will be presented elsewhere but, in general, strokes with high frequencies, low stroke angles, and high pitch amplitudes had the highest efficiency. This is not surprising given that a high pitch amplitude directs the resultant force more forward and a high frequency is necessary to achieve positive attack angles on the down stroke and negative angles on the up stroke. These optimal kinematics require both a high pitch magnitude and rate of rotation of the appendage, both of which are limited by musculoskeletal constraints in real animals. How these constraints limit performance remains to be investigated.

Second, the key to rowing, especially at low Re , is the ability of the appendage to generate more drag on the power stroke than recovery stroke. Animals that row at low Re create this asymmetry by greatly reducing paddle surface area and limb span (which reduces mean tangential velocity) during the recovery stroke (Fig. 4) (Nachtigall, 1974; Zaret and Kerfoot, 1980; Hessler, 1985; Fryer, 1991; Kohlhage and Yager, 1994; Vogel, 1994). In the water beetle, *Gyrinus*, appendage area is reduced 70 percent and the position of the limb's center of area from the limb base is re-

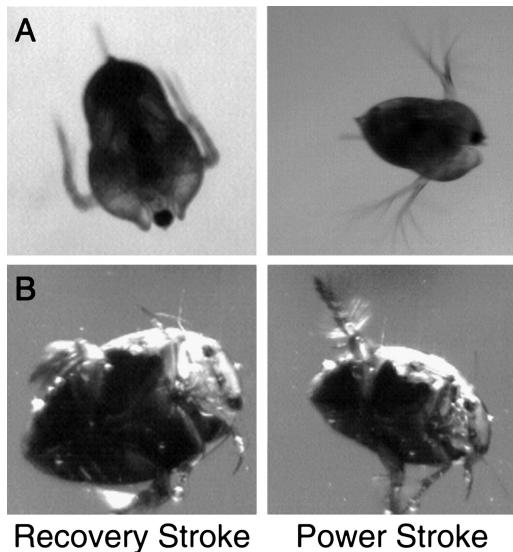


FIG. 4. The rowing strokes of a dytiscid beetle and water flea, *Daphnia sp.* The right-hand side of the figure illustrates the mid power-stroke with extended limbs and erect swimming hairs while the left-hand side illustrates the mid recovery-stroke with flexed limbs and collapsed swimming hairs.

duced 40 percent during the recovery stroke (Nachtigall, 1974). The ability to reduce area and span during the recovery stroke is intimately associated with the design of the propulsive limbs in small animals (Nachtigall, 1974). Importantly, both area and span reduction are passive responses to fluid dynamic loads, which makes this mechanism energetically cheap (Nachtigall, 1974).

To explore the effects of reduced appendage area on performance, a simulation was run with the chord length reduced by 50% during the recovery stroke. To account for the rapid collapse of most of the paddle surface area normal to the direction of appendage motion that occurs at the beginning of the recovery stroke in small, rowing animals, I allowed the rowing appendage to instantly rotate into a feathered orientation. The rotation into a broadside orientation at the beginning of the power stroke was retained. In this experiment, performance was reduced for the flapping appendage (results not shown), which is not surprising since this geometry generates thrust on both strokes. In contrast, η for the rowing appendage is substantially improved at all Re and J . Nevertheless, the flapping appendage is more efficient than the reduced-area rowing appendage at all Re and J .

To explore the combined effects of reduced area and span, a simulation was run with the recovery stroke chord lengths and span reduced 50% and 40%, respectively. The reduced span was modeled not by simply truncating the appendage, which would also reduce area, but by assigning the distal 40% of the appendage the recovery stroke kinematics of the element that is 60% from the base. This effectively models an appendage that flexes at the 60% span point and trails the distal 40% behind it (as in Fig. 4). As in the reduced area simulation, the rowing appendage instantly feathered at the beginning of the recovery stroke. Again, performance was reduced for the flapping appendage but greatly improved for the rowing appendage (Fig. 3). With low advance ratios, flapping tends to have higher performance than rowing, even at very low Re . For example, at $J = 0.2$, the efficiency of flapping exceeds that of reduced-area-and-span rowing when $Re > 4$. At $J = 0.4$, this Re increases to about 8. At $J = 1$, however, Re must exceed about 250 before flapping outperforms rowing (not shown).

While the experimental simulation of the virtual model suggests that rowing with reduced limb-span and paddle area on the recovery stroke is more effective than flapping at low Re , there is not a specific Re above which flapping is more effective and below which rowing is more effective (the cut-off Re). Instead, the simulation shows that the cut-off Re is a function of swimming speed. For hovering or swimming with low advance ratios, the cut-off Re is around 5, while for swimming with high advance ratios, the cut-off Re is around 250. With the exception of *Speleonectes*, the animals in Table 1 are moving at J s less than 0.6. The cut-off Re at $J = 0.6$ is about 20. Despite

the simplicity of the model, a cut-off Re of 20 is remarkably consistent with the available empirical data.

The model presented here does not include a number of factors that could influence the results, such as appendage shape (Blake, 1981; Daniel, 1988; Combes and Daniel, 2001), a squeeze force, the clap-and-fling, rotational optimization and wake-appendage interactions. Animals may generate thrust by closing a propulsive appendage against their body and squeezing, or accelerating, fluid in a net backwards direction (Daniel and Meyhöfer, 1989). At high Re ($>1,000$), there is no evidence of a significant squeeze force contributing to the force balance in the flapping appendage of a bird wrasse (Walker and Westneat, 1997) or the rowing appendage of a threespine stickleback (Walker, 1999). The clap-and-fling, in which instant high lift results from the expanding, low pressure region between a pair of separating appendages (Weis-Fogh, 1973), is known to operate down to at least Re 32 (Spedding and Maxworthy, 1986). In addition to its operation in some insects, it has been suggested that the flapping mechanism in the pteropod, *Clione limacina*, uses a clap-and-fling mechanism (Satterlie *et al.*, 1985). Rotational lift (Ellington, 1984), which results from the circulation created by an airfoil's own rotation around a spanwise axis (Fung, 1993), has been shown to be an important component in the force balance on model *Drosophila melanogaster* wings (Dickinson *et al.*, 1999) and could potentially work at low Re . While rotational lift was modeled, its contribution to the force balance was not optimized. Future work should attempt to find the lower Re limits of this important kinematic mechanism. Finally, Dickinson *et al.* (1999) have shown that wake-appendage interactions are important in the hovering flight of *D. melanogaster* but the influence of this mechanism at higher J or lower Re has not been investigated.

OTHER MORPHOLOGICAL CORRELATES

Morphologies associated with rowing and flapping illustrate many, beautiful evolutionary convergences. Within many different molluscs, arthropods and chordates, distally tapering, wing-shaped geometries are characteristic of flapping appendages, while distally expanded or paddle shaped appendages are characteristic of rowing appendages. To reduce the relative loss of energy at the appendage tips, flapping appendages should present relatively high aspect ratios and taper near the tip (Combes and Daniel, 2001), although the optimal shape is probably highly dependent on Re . In contrast, Blake (Blake, 1981) demonstrated that a triangle with a proximal apex and distal base is the most effective shape for rowing. Despite the relationship between appendage planform and dynamic shape, appendage planform is not strongly associated with Re across a broad range of taxa because of the multiple factors influencing the design of animal limbs (the multiple functions and preferred swimming speed hypotheses outlined above). Within groups, there may be stronger correlations between size and shape. Within

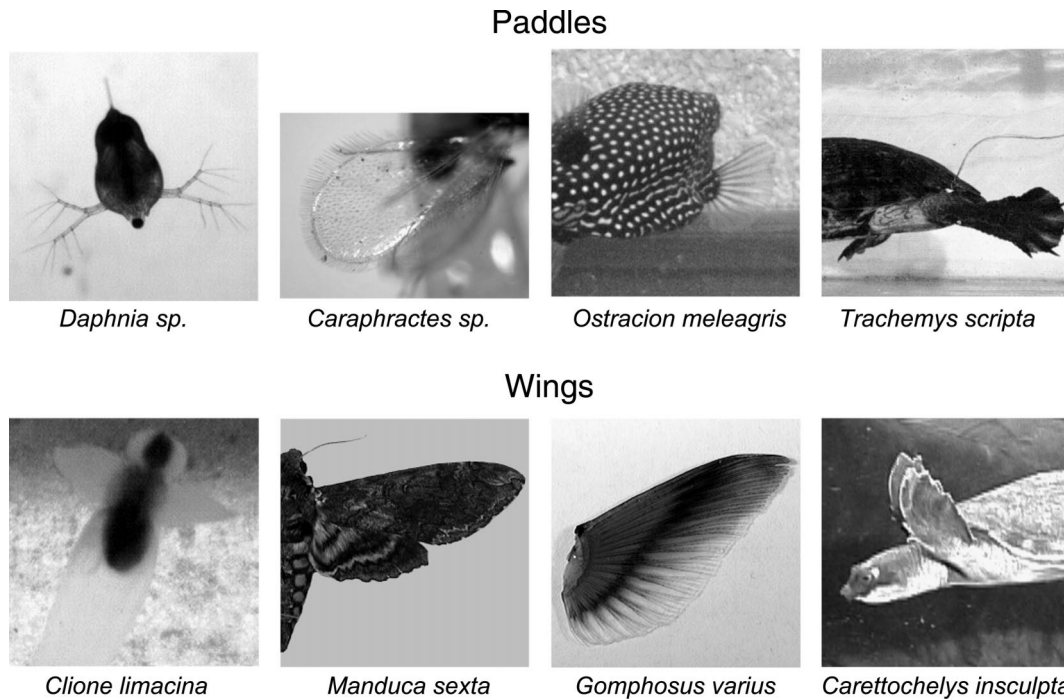


FIG. 5. Wings, fins, legs, and feet of swimming and flying animals illustrating convergence across both phyla (molluscs, arthropods, and chordates) and fluid media (air and water).

Hymenoptera, for example, wing aspect ratio decreases and the center of area moves distally as size decreases (Danforth, 1989).

At high Re , paddle-shaped appendages are formed from a continuous membrane but at low Re , the paddle-shape is often formed by hair-like structures radiating from a central shaft (Koehl, 1993; Vogel, 1994) (Fig. 5). Remarkably, hairy appendages are not confined to small, aquatic swimmers. Indeed, much of the aerodynamically active surface of the wings of the smallest insects, including members of the fairy flies (Hymenoptera: mymaridae) and feather-winged beetles (Coleoptera: Ptiliidae), is formed by hairs extending from a narrow, central membrane. It has been suggested that the smallest insects “swim” through air with a downward power stroke and upward recovery stroke (Thompson, 1917; Horridge, 1956; Bennett, 1972).

In response to fluid dynamic forces, the hairs on appendages are erect during the power stroke but collapse during the recovery stroke, with the result that the area and mean velocity of the appendage is much greater during the power than recovery stroke (Nachtigall, 1974). Using both mathematical and physical models, Koehl (Cheer and Koehl, 1987; Koehl, 1993; Loudon *et al.*, 1994) has shown that hairy appendages function as solid surfaces at $Re_{hair} < 10^{-2}$ but are leaky at $Re_{hair} > 1$, where Re_{hair} is based on hair diameter instead of chord length. Appendage hairs, then, provide an elegant, passive mechanism to reduce forces on the recovery stroke at low Re . Minute flying insects and the many swimming invertebrates within a certain size range can take additional advantage of this change

in the fluid mechanical properties of a hairy appendage. In fast forward motion, the peak velocities experienced by a rowing appendage, and the associated Re , are much less on the power stroke than on the recovery stroke. For example, an appendage that is 10 mm long, with hairs that are 2 mm long and 2.5 μm in diameter, oscillating at 5 Hz through a stroke angle of 120°, and attached to a body that is moving at 23 cm/sec will have maximum chord Re of 800, a maximum recovery stroke Re_{hair} of 0.8 and a maximum power stroke Re_{hair} of 0.05. Because the hairs are functioning in the critical Re range in this example, the hairy appendage should act like a solid paddle on the power stroke but a leaky paddle on the recovery stroke.

CONCLUSION

The combination of high viscous and low inertial forces challenges animals swimming or flying by oscillating appendages at $Re < 100$. The simulation experiment described here demonstrates the strong effect of Re on the mechanical efficiency of both rowing and flapping appendages at Re between 1 and 100. While the virtual model used in this paper is computationally trivial, it can easily accommodate features that were not explored in this study, including non-uniform swimming speeds, paddle leakiness and the squeeze force. Future work with the model should not only account for these features, but also the power limitations of wing, fin, leg and foot muscles. Despite the simplicity of the model, the results predict (or retrodict) both the exclusive use of a rowing stroke below a cut-off Re of about 20 and the reliance of a reduced

area and span during the recovery stroke of small rowing animals.

ACKNOWLEDGMENTS

This paper is dedicated to F. James Rohlf, a mentor with unexcelled abilities to teach a very special “geometric world view,” on the occasion of his 65th birthday. All of the fundamental tools that allowed the completion of this paper are due to his mentorship. I would like to thank the organizers of the symposium, M. Ashley-Ross, A. Gibb, and L. Ferry-Graham. Discussions with M. Dickinson, T. Daniel, and B. Wright helped to clarify some of these ideas but do not necessarily share some of the opinions expressed here. I especially thank two anonymous reviewers for providing constructive comments on the original manuscript. This work was supported by NSF award IBN-0119643, a grant from the Biosciences Research Institute of the University of Southern Maine, and ONR award N00014-99-1-0184 to M. W. Westneat and J. A. Walker.

REFERENCES

- Ahlborn, B., S. Chapman, R. Stafford, R. W. Blake, and D. G. Harper. 1997. Experimental simulation of the thrust phases of fast-start swimming of fish. *J. Exp. Biol.* 200:2301–2312.
- Anderson, J. M., K. Streitien, D. S. Barrett, and M. S. Triantafyllou. 1998. Oscillating foils of high propulsive efficiency. *J. Fluid Mech.* 360:41–72.
- Archer, R. D., J. Sapuppo, and D. S. Betteridge. 1979. Propulsion characteristics of flapping wings. *Aeronaut. J.* 83:355–371.
- Bellwood, D. R. and P. C. Wainwright. 2001. Locomotion in labrid fishes: Implications for habitat use and cross-shelf biogeography on the Great Barrier Reef. *Coral Reefs* 20:139–150.
- Bennett, L. 1972. Effectiveness and flight of small insects. *Ann. Entomol. Soc. Am.* 66:1187–1190.
- Blake, R. W. 1981. Influence of pectoral fin shape on thrust and drag in labriform locomotion. *J. Zool., London* 194:53–66.
- Blake, R. W. 1986. Hydrodynamics of swimming in the water boatman, *Cenocorixa bifida*. *Can. J. Zool.* 64:1606–1613.
- Chai, P., D. L. Altschuler, D. B. Stephens, and M. E. Dillon. 1999. Maximal horizontal flight performance of hummingbirds: Effects of body mass and molt. *Physiol. Biochem. Zool.* 72:144–155.
- Cheer, A. Y. L. and M. A. R. Koehl. 1987. Paddles and rakes: Fluid flow through bristled appendages of small organisms. *J. Theor. Biol.* 129:17–39.
- Combes, S. A. and T. L. Daniel. 2001. Shape, flapping and flexion: Wing and fin design for forward flight. *J. Exp. Biol.* 204:2073–2085.
- Danforth, B. N. 1989. The evolution of hymenopteran wings: The importance of size. *J. Zool., London* 218:247–276.
- Daniel, T., C. Jordan, and D. Grunbaum. 1992. Hydromechanics of swimming. In R. M. Alexander (ed.), *Mechanics of animal locomotion*, pp. 17–49. Springer-Verlag, Berlin.
- Daniel, T. L. 1984. Unsteady aspects of aquatic locomotion. *Amer. Zool.* 24:121–134.
- Daniel, T. L. 1988. Forward flapping flight from flexible fins. *Can. J. Zool.* 66:630–638.
- Daniel, T. L. and E. Meyhöfer. 1989. Size limits in escape locomotion of caridean shrimp. *J. Exp. Biol.* 143:245–265.
- Daniel, T. L. and P. W. Webb. 1987. Physical determinants of locomotion. In P. Dejours, L. Bolis, C. R. Taylor, and E. R. Weibel (eds.), *Comparative physiology: Life in water and on land*, pp. 343–369. Liviana Press, New York.
- Davenport, J. and A. Bebbington. 1990. Observations on the swimming and buoyancy of some thecosomatous pteropod gastropods. *J. Mol. Stud.* 56:487–497.
- Denny, M. W. 1988. *Biology and the mechanics of the wave-swept environment*. Princeton University Press, Princeton.
- Dickinson, M. H. 1996. Unsteady mechanisms of force generation in aquatic and aerial locomotion. *Amer. Zool.* 36:537–554.
- Dickinson, M. H. and K. G. Götz. 1993. Unsteady aerodynamic performance of model wings at low Reynolds numbers. *J. Exp. Biol.* 174:45–64.
- Dickinson, M. H., F.-O. Lehmann, and S. P. Sane. 1999. Wing rotation and the aerodynamic basis of insect flight. *Science* 284:1954–1960.
- Ellington, C. P. 1984. The aerodynamics of hovering insect flight. IV. Aerodynamic mechanisms. *Phil. Trans. R. Soc. London B* 305:79–113.
- Ellington, C. P., C. Van den Berg, and A. P. Willmott. 1996. Leading-edge vortices in insect flight. *Nature* 384:626–630.
- Emerson, S. B. and M. A. R. Koehl. 1990. The interaction of behavior and morphological change in the evolution of a novel locomotor type: “Flying” frogs. *Evolution* 44:1931–1946.
- Endler, J. A. 1986. *Natural selection in the wild*. Princeton University Press, Princeton.
- Endler, J. A. 1995. Multiple-trait coevolution and environmental gradients in guppies. *TREE* 10:22–29.
- Ennos, A. R. 1989. The kinematics and aerodynamics of the free flight of some diptera. *J. Exp. Biol.* 142:49–85.
- Farley, C. T. and T. A. McMahon. 1992. Energetics of walking and running—insights from simulated reduced gravity experiments. *J. App. Physiol.* 73:2709–2712.
- Fish, F. E. 1993. Influence of hydrodynamic design and propulsive mode on mammalian swimming energetics. *Aust. J. Zool.* 42:79–101.
- Fish, F. E. 1996. Transitions from drag-based to lift-based propulsion in mammalian swimming. *Amer. Zool.* 36:628–641.
- Freymuth, P. 1988. Propulsive vortical signature of plunging and pitching airfoils. *AIAA J.* 26:881–883.
- Fryer, G. 1991. Functional morphology and the adaptive radiation of the Daphniidae (Branchiopoda: Anomopoda). *Phil. Trans. R. Soc. London B* 331:1–99.
- Fuiman, L. A. and R. S. Batty. 1997. What a drag it is getting cold: Partitioning the physical and physiological effects of temperature on fish swimming. *J. Exp. Biol.* 200:1745–1755.
- Fulton, C. J., D. R. Bellwood, and P. C. Wainwright. 2001. The relationship between swimming ability and habitat use in wrasses (Labridae). *Mar. Biol.* 139:25–33.
- Fung, Y. C. 1993. *An introduction to the theory of aeroelasticity*. Dover, New York.
- Garland, T., Jr. and S. C. Adolph. 1994. Why not to do two-species comparative studies: Limitations on inferring adaptation. *Physiol. Zool.* 67:797–828.
- Harbison, G. R. 1992. Observations on the swimming and buoyancy of *Cymbulia peroni* (Gastropoda: Thecosomata) made from a submersible. *J. Mar. Biol. Ass. U.K.* 72:435–446.
- Hessler, R. R. 1985. Swimming in Crustacea. *Trans. Roy. Soc. Edinburgh* 76:115–122.
- Horridge, G. A. 1956. The flight of very small insects. *Nature* 178:1334–1335.
- Jayne, B. C. and A. F. Bennett. 1989. The effect of tail morphology on locomotor performance of snakes: A comparison of experimental and correlative methods. *J. Exp. Zool.* 252:126–133.
- Johnson, T. P., A. J. Cullum, and A. F. Bennett. 1998. Partitioning the effects of temperature and kinematic viscosity on the c-start performance of adult fishes. *J. Exp. Biol.* 201:2045–2051.
- Kato, N. 1999. Hydrodynamic characteristics of mechanical pectoral fin. *J. Fluids Eng.* 121:605–613.
- Kingsolver, J. G. and M. A. R. Koehl. 1985. Aerodynamics, thermoregulation, and the evolution of insect wings: Differential scaling and evolutionary change. *Evolution* 39:488–504.
- Koehl, M. A. R. 1993. Hairy little legs: Feeding, smelling, and swimming at low Reynolds numbers. *Contemp. Math.* 141:33–47.
- Kohlhage, K. 1994. The economy of paddle-swimming: The role of added waters and viscosity in the locomotion of *Daphnia magna*. *Zool. Beitr.* 35:47–54.

- Kohlhage, K. and J. Yager. 1994. An analysis of swimming in remipede crustaceans. *Phil. Trans. R. Soc. Lond. B* 346:213–221.
- Kuethle, A. M. and C.-Y. Chow. 1986. *Foundations of aerodynamics*. John Wiley & Sons, New York.
- Law, T. C. and R. W. Blake. 1996. Comparison of fast-start performances of closely related, morphologically distinct threespine sticklebacks (*Gasterosteus* spp.). *J. Exp. Biol.* 199:2595–2604.
- Leroi, A. M., M. R. Rose, and G. V. Lauder. 1994. What does the comparative method reveal about adaptation? *Am. Nat.* 143:381–402.
- Loudon, C., B. A. Best, and M. A. R. Koehl. 1994. When does motion relative to neighboring surfaces alter the flow through arrays of hairs? *J. Exp. Biol.* 193:233–254.
- McHenry, M. J., C. A. Pell, and J. H. Long, Jr. 1995. Mechanical control of swimming speed: Stiffness and axial wave form in undulating fish models. *J. Exp. Biol.* 198:2293–2305.
- Morris, M. J., G. Gust, and J. J. Torres. 1985. Propulsion efficiency and cost of transport for copepods: A hydromechanical model of crustacean swimming. *Mar. Biol.* 86:283–295.
- Morris, M. J., K. Kohlhage, and G. Gust. 1990. Mechanics and energetics of swimming the small copepod *Acanthocylops robustus* (Cylopoida). *Mar. Biol.* 107:83–91.
- Morton, J. E. 1954. The biology of *Limacina retroversa*. *J. Mar. Biol. Ass. U.K.* 33:297–312.
- Morton, J. E. 1958. Observations on the gymnosomatous pteropod *Clione limacina*. *J. Mar. Biol. Ass. U.K.* 37:287–297.
- Nachtigall, W. 1974. Locomotion: Mechanics and hydrodynamics of swimming in aquatic insects. In M. Rockstein (ed.), *The physiology of Insecta*, pp. 381–432. Academic Press, New York.
- Norberg, R. A. 1972. Flight characteristics of two plume moths, *Alucita pentadactyla* L. and *Orneodes hexadactyla* L. (Microlepidoptera). *Zoo. Script.* 1:241–246.
- Olsson, M., R. Shine, and E. Bak-Olsson. 2000. Locomotor impairment of gravid lizards: Is the burden physical or physiological? *J. Evol. Biol.* 13:263–268.
- Plotnick, R. E. 1985. Lift based mechanisms for swimming in eurypterids and portunid crabs. *Trans. Roy. Soc. Edinburgh* 76:325–337.
- Sato, M. and A. Azuma. 1997. The flight performance of a damselfly *Ceriatrigon melanurum* Selys. *J. Exp. Biol.* 200:1765–1779.
- Satterlie, R. A., M. LaBarbera, and A. N. Spencer. 1985. Swimming in the pteropod mollusc, *Clione limacina*. *J. Exp. Biol.* 116:189–204.
- Satterlie, R. A., T. P. Norekian, and K. J. Robertson. 1997. Startle phase of escape swimming is controlled by pedal motoneurons in the pteropod mollusk *Clione limacina*. *J. Neurophysiol.* 77:272–280.
- Seibel, B. A., E. V. Thuesen, and J. J. Childress. 1998. Flight of the vampire: Ontogenetic gait-transition in *Vampyroteuthis infernalis* (Cephalopoda: Vampyromorpha). *J. Exp. Biol.* 201:2413–2424.
- Shyy, W., M. Berg, and D. Ljungqvist. 1999. Flapping and flexible wings for biological and micro air vehicles. *Prog. Aero. Sci.* 35:455–506.
- Sinervo, B. and A. L. Basolo. 1996. Testing adaptation using phenotypic manipulations. In M. R. Rose and G. V. Lauder (eds.), *Adaptation*, pp. 149–185. Academic Press, San Diego.
- Sinervo, B., R. Hedges, and S. C. Adolph. 1991. Decreased sprint speed as a cost of reproduction in the lizard *Sceloporus accidentialis*: variation among populations. *J. Exp. Biol.* 155:323–336.
- Spedding, G. R. and T. Maxworthy. 1986. The generation of circulation and lift in a rigid two-dimensional fling. *J. Fluid. Mech.* 165:247–272.
- Srygley, R. B. and J. G. Kingsolver. 2000. Effects of weight loading on flight performance and survival of palatable Neotropical *Artantia fatima* butterflies. *Biol. J. Linnean Soc.* 70:707–725.
- Thom, A. and P. Swart. 1940. Forces on an airfoil at very low speeds. *J. Roy. Aero. Soc.* 44:761–770.
- Thompson, D. A. W. 1917. *On growth and form*. Cambridge University Press, Cambridge.
- Tobalske, B. W. 2000. Biomechanics and physiology of gait selection in flying birds. *Physiol. Biochem. Zool.* 73:736–750.
- Veasey, J. S., D. C. Houston, and N. B. Metcalfe. 2000. Flight muscle atrophy and predation risk in breeding birds. *Funct. Ecol.* 14:115–121.
- Vogel, S. 1994. *Life in moving fluids*, 2nd ed. Princeton University Press, Princeton.
- Walker, J. A. 1999. Pectoral fin rowing is a drag. *Amer. Zool.* 38:18A.
- Walker, J. A. and M. W. Westneat. 1997. Labriform propulsion in fishes: Kinematics of flapping aquatic flight in the bird wrasse *Gomphosus varius* (Labridae). *J. Exp. Biol.* 200:1549–1569.
- Walker, J. A. and M. W. Westneat. 2000. Mechanical performance of aquatic rowing and flying. *Proc. R. Soc. London B* 267:1875–1881.
- Walker, J. A. and M. W. Westneat. 2002. Performance limits of labriform propulsion and correlates with fin shape and motion. *J. Exp. Biol.* 205:177–187.
- Webb, P. W. and D. Weihs. 1986. Functional locomotor morphology of early life history stages of fishes. *Trans. Am. Fish. Soc.* 115:115–127.
- Weis-Fogh, T. 1973. Quick estimates of flight fitness in hovering animals, including novel mechanisms for lift production. *J. Exp. Biol.* 59:169–230.
- Williams, T. A. 1994. A model of rowing propulsion and the ontogeny of locomotion in *Artemia* larvae. *Biol. Bull.* 187:164–173.
- Zaret, R. E. and W. C. Kerfoot. 1980. The shape and swimming technique of *Bosmina longirostris*. *Limnol. Oceanogr.* 25:126–133.